

## Isolation of homogeneous fluorophores obtained at different stages of hydrothermal synthesis of carbon dots

© K.A. Laptinskiy<sup>1,2</sup>, A.M. Verval'd<sup>1</sup>, A.A. Korepanova<sup>1</sup>, T.A. Dolenko<sup>1</sup>

<sup>1</sup> Moscow State University, Moscow, Russia

<sup>2</sup> Skobeltsyn Institute of Nuclear Physics, Moscow State University, Moscow, Russia

e-mail: laptinskiy@physics.msu.ru

Received May 05, 2025

Revised July 07, 2025

Accepted October 24, 2025

The isolation of carbon dot fractions obtained at different stages of hydrothermal synthesis from citric acid and ethylenediamine is discussed. Gel electrophoresis was used for the isolation, resulting in the isolation of up to five different carbon dot fractions formed at the same stage of hydrothermal synthesis. The optical properties of each isolated fraction were analyzed using photoluminescence spectroscopy, photometry, time-resolved spectroscopy, and IR absorption spectroscopy.

**Keywords:** carbon dots, fractionation, electrophoresis, fluorophores.

DOI: 10.61011/EOS.2025.10.62563.8041-25

### Introduction

Carbon dots (CDs), the first representatives of which were mentioned in 2004 [1], are typically described as zero-dimensional quasi-spherical nanoparticles up to 10 nm in size with a carbon core. However, for some CDs this carbon core may not exist in the strict sense — in bottom-up synthesis CDs may be a fully polymeric structure [2]. Precisely such nanoparticles can be synthesized using one of the most popular methods — hydrothermal synthesis. This simple, inexpensive, and easily scalable method enables the production of a wide variety of CDs by varying the type and concentrations of molecular precursors as well as synthesis parameters such as time and temperature [3].

A series of processes involving precursors has been identified in the hydrothermal synthesis of CDs: dehydration, polymerization, carbonization, and passivation/doping with organic molecules [4]. It is assumed that during these transformations, precursors gradually convert from individual molecules into bulk polymers, which then densify to form and progressively grow the carbon core of nanoparticles, passivated or doped with various functional groups, individual molecules, or atoms.

Carbon dots attract attention due to their stable and bright photoluminescence (PL) [5], the origin of which depends on their structure: the carbon core (quantum confinement, defects) or the surface (molecular luminophores, functional groups) [6]. Photoluminescence is sensitive to temperature [7], pH [8], and metal ions [9,10], enabling the development of nanosensors. The highest PL quantum yield (up to ~ 100%) is demonstrated by hydrothermally synthesized CDs, particularly polymeric ethylenediamine/citric acid CDs [11,12]. However, synthesis yields a polydisperse mixture requiring purification and fractionation [13]. For example, electrophoresis has shown that citric acid deriva-

tives do not form a CD core [13] and the staged nature of synthesis affects optical properties [14].

This work presents the results of fractionating CDs synthesized hydrothermally from citric acid (CA) and ethylenediamine (EDA) at different synthesis stages. Fractionation was performed using horizontal electrophoresis, with each fraction characterized in detail using a set of methods.

### Materials and methods

Carbon dots were synthesized via the hydrothermal method. CA (monohydrate, Ruskhim, analytical grade) and EDA (produced by AO „EKOS-1“, extra pure) were used as precursors. To achieve a 1:1 molar ratio of precursors, 10.53 g CA were mixed with 3.35 mL EDA and diluted with deionized water (Millipore Milli-Q) to a volume of 500 mL, resulting in a concentration of 0.1 M for each precursor. Different stages of CDs' hydrothermal synthesis were achieved under the following conditions: autoclaves containing the reaction mixture were held in a Sputnik muffle furnace (Russia) for 30 min at 80 °C (stage 2), 2 h at 120 °C (stage 3), 4 h at 140 °C (stage 4), and 6 h at 200 °C (stage 5). After the specified thermal exposure time, the autoclaves were removed from the furnace and cooled naturally to room temperature.

For CD fractionation, horizontal electrophoresis was performed in a 2% (w/v) agarose gel (diaGene, Russia) on a 20 mM NaCl buffer compatible with infrared (IR) spectroscopy. The procedure involved preparing the gel (heating to 130 °C until transparent, then cooling to 55 °C), forming 13 wells, loading 20 μL of CD samples, and electrophoresis on an SVL-2 system (China) with an „Elf-8“ power supply (DNA-Technology, Russia).

PL spectra of CDs obtained at different hydrothermal synthesis stages and of various CD fractions were recorded us-

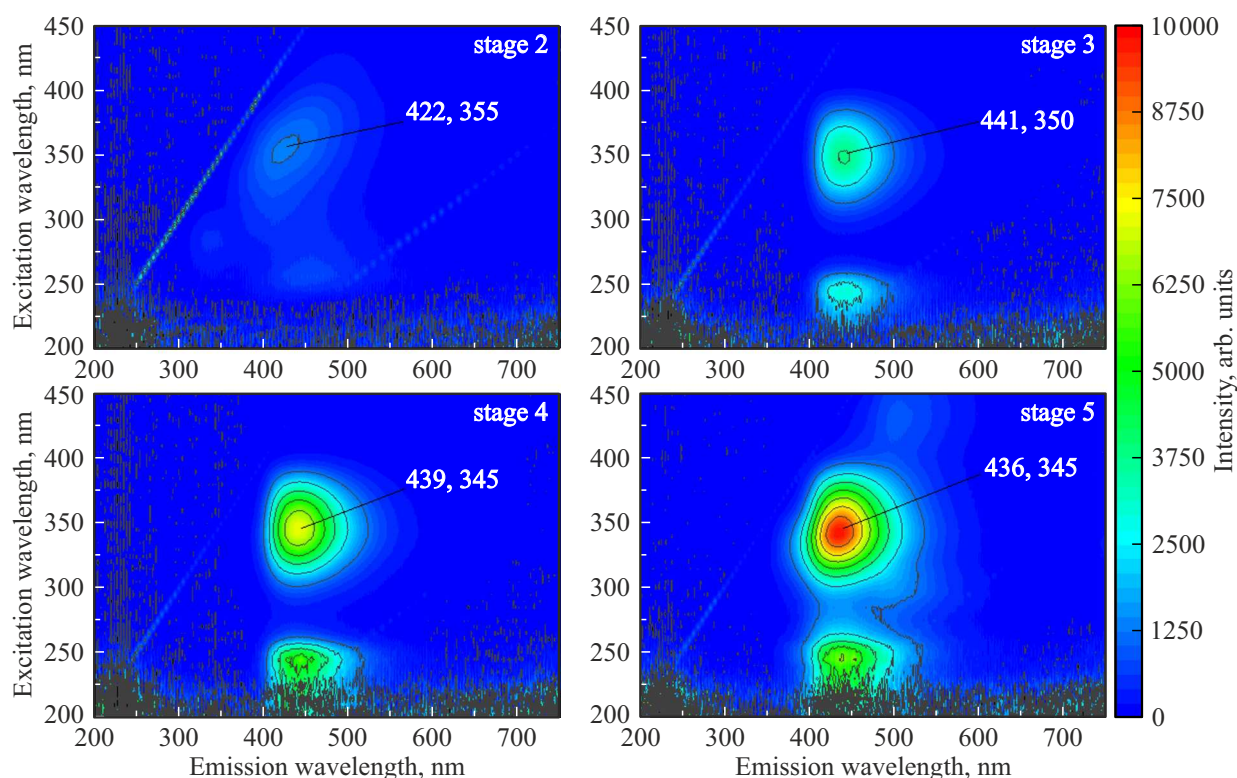


**Figure 1.** Excitation-emission PL matrices of CDs obtained at different stages of hydrothermal synthesis.

**Table 1.** Characterization results for CDs obtained at different stages of hydrothermal synthesis

Synthesis stage	LQY, %	Zeta potential, mV	PL lifetime, ns
5	$43 \pm 2$	$-18.7 \pm 12.4$	3.0 (12%), 14.4 (88%)
4	$77 \pm 4$	$-8.1 \pm 1.7$	15.0 (100%)
3	$92 \pm 5$	$-0.5 \pm 0.4$	14.8 (100%)
2	$10 \pm 1$	$-0.7 \pm 0.1$	3.0 (51%), 10.9 (49%)

ing a Shimadzu RF-6000 spectrofluorimeter (Japan); optical density spectra of CDs were obtained with a Shimadzu UV-1800 spectrophotometer (Japan). Luminescence quantum yield (LQY) values were determined using the reference dye method, with quinine sulfate in aqueous sulfuric acid (concentration  $\text{H}_2\text{SO}_4$  of 0.05 M) as the reference dye. The LQY determination method is described in detail in [15]. PL decay kinetics were acquired using a setup consisting of a picosecond laser (excitation wavelength 373 nm, repetition rate 5 MHz, pulse duration 40 ps), a DSC900PS single-photon counting system (Zolix, China), and an OmniFluo 900 LPS spectrofluorimeter (Zolix, Russia). Luminescence decay kinetics were recorded at a PL emission wavelength of 440 nm (corresponding to the fluorescence maximum of the CDs). Zeta potentials were measured using a Malvern ZetaSizer Nano ZS instrument (UK). IR absorption spectra of CDs and their fractions were recorded using a Bruker INVENIO R FTIR spectrometer

(Germany) in the attenuated total reflectance (ATR) mode. To do this,  $10 \mu\text{L}$  of sample was placed on the ATR diamond plate and dried with a stream of room air for 8 min. Spectral processing involved smoothing (Savitzky-Golay method over 10 points) and baseline subtraction (adaptive baseline, roughness — 22%, offset — 0). Spectral processing was performed in Spectragryph software [16].

## Results and Discussion

Figure 1 shows the excitation-emission PL matrices of CDs. The data indicate that PL of CDs obtained at different synthesis stages differs. Shifts are observed in the positions of the main PL emission and excitation maxima: the emission maximum position varies in the range 422 – 441 nm while the excitation maximum position varies in the range 345 – 355 nm. The synthesized CDs also differ in LQY values (Table 1). The presence of multiple PL peaks

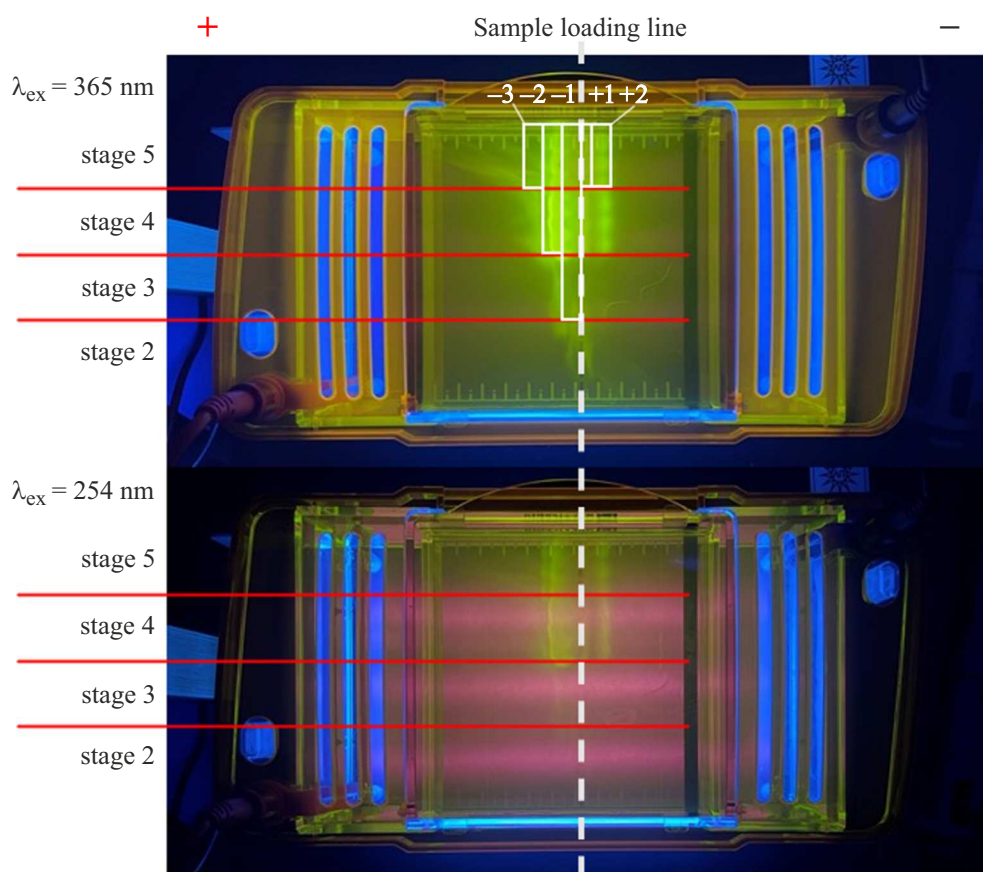


**Figure 2.** Fractionation of CDs obtained at different stages of hydrothermal synthesis. The white dashed line corresponds to the line formed by the wells into which samples were loaded. White rectangles indicate the template for the extraction of gel fragments.

suggests the formation of several luminophores within each synthesis stage. To isolate different CD fractions from each stage, horizontal electrophoresis was employed.

Different CD fractions were visualized with the help of a UV-6 transilluminator (Miulab, China), which provides the uniform gel illumination at wavelengths of 254 or 365 nm (Fig. 2). Initial electrophoresis conditions: current 165 mA, voltage 100 V, power 16.5 W, gel temperature 21 °C; at the end of the experiment: current 125 mA, voltage 47 V, power 5.9 W, gel temperature 29 °C. Fractionation time was 65 min. After electrophoresis, gel pieces containing the isolated CD fractions were excised from the bulk gel and placed into Eppendorf tubes. These gel pieces were then crushed and immersed in water to release the CD fractions from the agarose gel. To remove gel remnants, an Eppendorf MiniSpin centrifuge (Germany) was used at 13400 rpm (12100 g) for 30 min. The supernatant was collected and used in subsequent studies.

From Fig. 2, it is evident that applying voltage to the gel causes separation of the CD samples and multidirectional migration of fractions. Notably, different numbers of fractions were isolated from CDs synthesized at different stages: the highest number (five) from stage 5 CDs, the lowest (one) from stage 3 CDs. Each isolated fraction was characterized, with results shown in Figs. 3, 4 and Table 2.

As expected, the excitation-emission PL matrices of different fractions differ from one another. For example, for the five fractions of stage 5 CDs, the emission maximum position varies in the range 426 – 452 nm, and the excitation maximum position in the range 340 – 350 nm (Fig. 3). The isolated luminophores exhibit different LQY values, which can differ by approximately a factor of two for fractions from the same synthesis stage (Table 2). Comparing the LQY of the initial stage 3 CD sample ( $LQY = 92 \pm 5\%$ ) with its single isolated fraction 3-1 ( $LQY = 18 \pm 1\%$ ) suggests that the majority of the stage 3 product consists of the low-LQY isolated fraction; however, luminophores with very intense PL are already present, likely not captured in the isolated fraction volume.

The obtained luminescence decay kinetics for each fraction indicate the presence of at least two distinct luminophores in all isolated CD fractions, with PL lifetimes of  $\sim 3.5$  and  $\sim 12.5$  ns. The ratio of these two luminophores varies across different fractions. Thus, the smallest proportion of short-lived luminophores is observed in sample 5 – 3, i.e., the most charged and smallest in size, which enables this fraction to migrate farther within the agarose gel volume. At the same time, luminophores with characteristic lifetimes of  $\sim 20$  ns are found in different CD fractions (in sample 5 + 1).

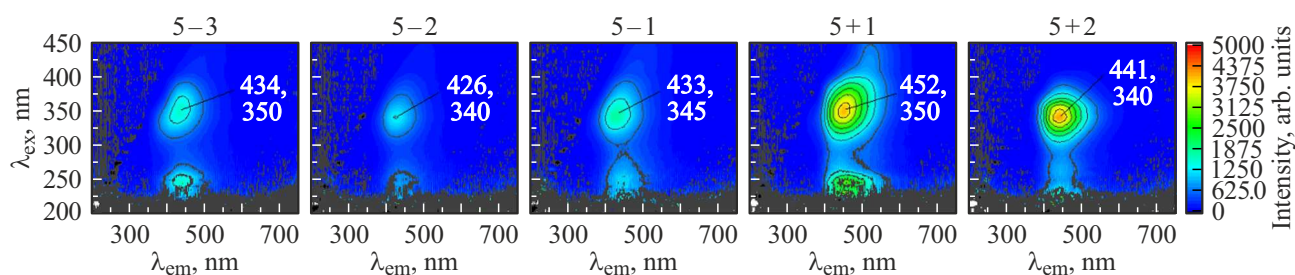


**Figure 3.** Excitation-emission PL matrices of different fractions of CDs obtained by electrophoresis of a CD sample synthesized for 6 h at 200 °C (stage 5).

**Table 2.** Characterization results for isolated CD fractions obtained at different stages of hydrothermal synthesis

Synthesis stage	Fraction	LQY, %	Zeta potential, mV	PL lifetime, ns
5	-3	15 ± 1	-49.8 ± 14.3	3.5 (26%), 13.7 (74%)
5	-2	21 ± 1	-36.7 ± 10.7	3.7 (37%), 12.4 (63%)
5	-1	19 ± 1	-12.2 ± 4.5	3.1 (39%), 12.1 (61%)
5	+1	26 ± 1	-4.0 ± 3.0	3.3 (17%), 19.7 (83%)
5	+2	40 ± 2	-3.0 ± 3.1	2.9 (43%), 10.0 (57%)
4	-2	50 ± 2	-14.4 ± 3.6	3.5 (35%), 12.2 (65%)
4	-1	29 ± 1	-3.6 ± 2.8	8.4 (80%), 12.6 (20%)
3	-1	18 ± 1	-3.0 ± 3.3	3.5 (42%), 10.2 (58%)

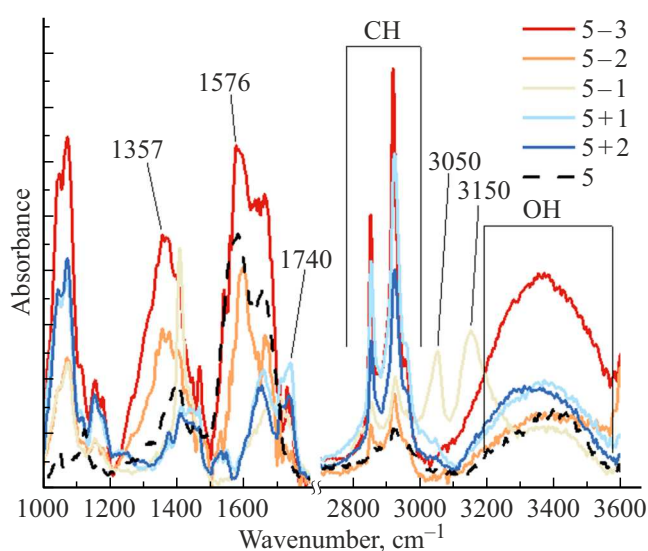


**Figure 4.** IR spectra of a CD sample synthesized for 6 h at 200 °C (black dashed line, stage 5) and different CD fractions obtained by electrophoresis of the sample.

As evident from Fig. 4, the IR spectra of different fractions isolated by electrophoresis of stage 5 CDs differ substantially from one another. For instance, in the IR spectra of fractions migrating toward the positive pole

(samples 5 - 3, 5 - 2), a band appears around 1357 cm<sup>-1</sup>, attributed to deformation vibrations in CH<sub>3</sub>-groups [17], and a band around 1576 cm<sup>-1</sup> due to C=N vibrations [18]. Notably, the IR spectrum of fraction 5-1 differs from the others by featuring a narrow spectral band at 1408 cm<sup>-1</sup> (corresponding to vibrations of the deprotonated form of carboxyl groups [19]), as well as bands with maxima around 3050 cm<sup>-1</sup> (presumably corresponding to C=C vibrations [19]) and 3150 cm<sup>-1</sup> (attributed to hydroxyl-N hydrogen bonding [20]). Precise analysis of the IR absorption spectra of all isolated fractions, combined with other methods (e.g., XPS), could enable determination of the structural formulas of individual CD luminophores.

## Conclusion

Successful fractionation of CDs obtained at different stages of hydrothermal synthesis from CA and EDA has been demonstrated. The CD fractions differ in their physicochemical, optical, and structural properties. Specifically, LQY values of different CD fractions vary by factors of several times (for synthesis stage 5, the lowest value is 15%, the highest — 40%), and substantial differences are observed in the IR spectra of different fractions. Horizontal gel electrophoresis proved effective for isolating CD fractions and homogeneous luminophores possessing

distinct properties, which could potentially be more efficient for specific applied tasks.

### Acknowledgments

A.A. Korepanova expresses gratitude to the Basis Foundation for the Development of Theoretical Physics and Mathematics for supporting the research project № 24-2-1-109-1. The work utilized equipment from the MSU Accelerator Complex Shared Facility Center (FTIR spectrometer acquired under the MSU Development Program (Agreement № 65 dated 04.10.2021)). Some experimental results used in this work were obtained using equipment from the MSU Center for Quantum Technologies Shared Facility Center (high-speed luminescence decay kinetics analysis system acquired under the MSU Development Program (Contract № 231 dated June 6, 2023)).

### Funding

The research was conducted under the state assignment of Lomonosov Moscow State University.

### Conflict of interest

The authors declare that they have no conflict of interest.

### References

- [1] X. Xu et al. *J. Am. Chem. Soc.*, **126**, 12736 (2004). DOI: 10.1021/ja040082h
- [2] X. Zheng et al. *Mater. Lett.*, **238**, 22 (2019). DOI: 10.1016/j.matlet.2018.11.147
- [3] H. Liu et al. *Coord. Chem. Rev.*, **498**, 215468 (2024). DOI: 10.1016/j.ccr.2023.215468
- [4] A.M. Vervalde et al. *ZhTF*, **95** (2), 232 (2025) (in Russian). DOI: 10.61011/JTF.2025.02.59713.280-24
- [5] A. Selva Sharma, N.Y. Lee. *Analyst*, **149**, 4095 (2024). DOI: 10.1039/D4AN00630E
- [6] D. Ozyurt et al. *Carbon Trends*, **12**, 100276 (2023). DOI: 10.1016/j.cartre.2023.100276
- [7] O.E. Sarmanova et al. *Spectrochim. Acta A*, **258**, 119861 (2021). DOI: 10.1016/j.saa.2021.119861
- [8] C. Yu et al. *J. Phys. Chem. C*, **127**, 3176 (2023). DOI: 10.1021/acs.jpcc.2c06449
- [9] J. Dhariwal, G.K. Rao, D. Vaya. *RSC Sustainability*, **2**, 11 (2024). DOI: 10.1039/D3SU00375B
- [10] A.M. Vervalde et al. *J. Phys. Chem. C*, **127** (44), 21617 (2023). DOI: 10.1021/acs.jpcc.3c05231
- [11] N.A.S. Omar et al. *Nanomater.*, **12**, 2365 (2022). DOI: 10.3390/nano12142365
- [12] M. Zhang et al. *Opt. Mater.* **135**, 113311 (2023). DOI: 10.1016/j.optmat.2022.113311
- [13] A.A. Kokorina et al. *Sci. Rep.*, **9**, (2019). DOI: 10.1038/s41598-019-50922-6
- [14] A.M. Vervalde et al. *Carbon Trends*, **19**, 100452 (2025). DOI: 10.1016/j.cartre.2025.100452
- [15] M.Yu. Khmeleva, K.A. Laptinskiy, T.A. Dolenko. *Opt. i spektr.*, **131**, 797 (2023) (in Russian). DOI: 10.21883/os.2023.06.55913.104-23
- [16] F. Menges. *Spectragryph — optical spectroscopy software. Version 1.2.15* (2020). <http://www.effemm2.de/spectragryph/>
- [17] L.P. Barros et al. *Polym. Test.*, **103**, 107350 (2021). DOI: 10.1016/j.polymertesting.2021.107350
- [18] T.S. Sych et al. *Nanoscale Adv.*, **1**, 3579 (2019). DOI: 10.1039/C9NA00112C
- [19] A. Gholampour et al. *ACS Appl. Mater. Interfaces*, **9**, 43275 (2017). DOI: 10.1021/acsami.7b16736
- [20] X. Wang, X. He, X. Wang. *Appl. Sci.*, **13**, 5162 (2023). DOI: 10.3390/app13085162

*Translated by J.Savelyeva*